REGULAR ARTICLE

blood advances

Bleeding diathesis in mice lacking JAK2 in platelets

Nathan Eaton,[1,2] Saravanan Subramaniam,[1] Marie L. Schulte,[1] Caleb Drew,[1] David Jakab,[1] Sandra L. Haberichter,[1,3,4] Hartmut Weiler,[1,5] and Hervé Falet[1,2]

[1]Versiti Blood Research Institute, Milwaukee, WI; [2]Department of Cell Biology, Neurobiology, and Anatomy and [3]Department of Pediatrics, Medical College of Wisconsin, Milwaukee, WI; [4]Children's Research Institute, Children's Wisconsin, Milwaukee, WI; and [5]Department of Physiology, Medical College of Wisconsin, Milwaukee, WI

Key Points

- Mice lacking the tyrosine kinase JAK2 in platelets develop a bleeding diathesis, despite severe thrombocytosis.
- JAK2 is required for immunoreceptor tyrosine-based activation motif signaling and platelet hemostatic function in mice.

The tyrosine kinase JAK2 is a critical component of intracellular JAK/STAT cytokine signaling cascades that is prevalent in hematopoietic cells, such as hematopoietic stem cells and megakaryocytes (MKs). Individuals expressing the somatic *JAK2* V617F mutation commonly develop myeloproliferative neoplasms (MPNs) associated with venous and arterial thrombosis, a leading cause of mortality. The role of JAK2 in hemostasis remains unclear. We investigated the role of JAK2 in platelet hemostatic function using *Jak2*$^{fl/fl}$ *Pf4-Cre* (*Jak2*$^{Plt-/-}$) mice lacking JAK2 in platelets and MKs. *Jak2*$^{Plt-/-}$ mice developed MK hyperplasia and splenomegaly associated with severe thrombocytosis and bleeding. This notion was supported by failure to occlude in a ferric chloride carotid artery injury model and by a cremaster muscle laser-induced injury assay, in which *Jak2*$^{Plt-/-}$ platelets failed to form stable thrombi. *Jak2*$^{Plt-/-}$ platelets formed thrombi poorly after adhesion to type 1 collagen under arterial shear rates. *Jak2*$^{Plt-/-}$ platelets spread poorly on collagen under static conditions or on fibrinogen in response to the collagen receptor GPVI-specific agonist, collagen-related peptide (CRP). After activation with collagen, CRP, or the CLEC-2 agonist rhodocytin, *Jak2*$^{Plt-/-}$ platelets displayed decreased α-granule secretion and integrin αIIbβ3 activation or aggregation, but showed normal responses to thrombin. *Jak2*$^{Plt-/-}$ platelets had impaired intracellular signaling when activated via GPVI, as assessed by tyrosine phosphorylation. Together, the results show that JAK2 deletion impairs platelet immunoreceptor tyrosine-based activation motif signaling and hemostatic function in mice and suggest that aberrant JAK2 signaling in patients with MPNs affects GPVI signaling, leading to hemostatic platelet function.

Introduction

The protein tyrosine kinase JAK2 is a member of the Janus kinase family, which includes JAK1, JAK2, JAK3, and Tyk2. JAK2 is most commonly associated with its role in cytokine signaling, which is prevalent in a variety of cell types and is required in numerous physiological processes, including hematopoiesis, immunity, inflammation, and tumorigenesis.[1] The interaction between the cytokine receptor Mpl and its cognate ligand, thrombopoietin (TPO), induces its oligomerization followed by JAK2 phosphorylation and activation, instigating the recruitment of signal transducer and activator of transcription (STAT) proteins and their subsequent translocation to the nucleus to induce transcription.[2]

Essential thrombocythemia (ET), myelofibrosis (MF), and polycythemia vera (PV) are Philadelphia chromosome-negative myeloproliferative neoplasms (MPNs) that arise from mutually exclusive somatic mutations in the *JAK2*, *MPL*, or *CALR* genes within the bone marrow hematopoietic stem cell (HSC)

Submitted 24 July 2020; accepted 14 April 2021; published online 3 August 2021.
DOI 10.1182/bloodadvances.2020003032.

For original data, please contact Hervé Falet at hfalet@versiti.org.

The full-text version of this article contains a data supplement.

compartment and result in constitutive cytokine signaling via the JAK/STAT pathway and clonal expansion of HSCs.[3,4] Structurally, JAK2 comprises an N-terminal FERM domain, an atypical SH2 domain, an autoinhibitory pseudokinase domain, and a C-terminal kinase domain, where the pseudokinase domain is critical in autoinhibiting JAK2 kinase activity.[5] Activating somatic mutations within the *JAK2* gene, including the mutation V617F and mutations in exon 12, which encodes the pseudokinase domain, can be found in more than half of patients with ET and MF and in >90% of patients with PV, illustrating a critical role for JAK2 in the development of MPN.[6]

Patients with MPNs are at increased risk of thrombosis/thromboembolism and major disease-related bleeding complications.[7-11] Because of the morbidity and mortality related to these events, antiplatelet and/or anticoagulant agents are commonly used as primary and/or secondary prophylaxis. Individuals harboring the *JAK2* V617F mutation show increased risk of thrombotic events, compared with individuals with *CALR* mutations,[6,11,12] lending credence to the notion of a highly complex role of JAK2 in hemostasis.

Recent studies in knockin mice expressing *JAK2* V617F show that hyperactive JAK2 can lead to diminished, normal, or enhanced platelet function and hemostasis, regardless of the number of circulating platelets.[13-16] Combined with the clinical observations derived from patients carrying *JAK2* V617F, the human and mouse data suggest that JAK2 expression and activity affect the degree of hemostatic potential. However, the cellular mechanisms by which JAK2 expression and activity regulate platelet hemostatic function remain unclear.

In this study, the role of platelet JAK2 was examined in $Jak2^{fl/fl}$ *Pf4-Cre* ($Jak2^{Plt-/-}$) mice lacking JAK2 in platelets and megakaryocytes (MKs) and presenting an expansion of MK-affiliated hematopoietic progenitors and subsequent severe thrombocytosis.[17] Our data show that $Jak2^{Plt-/-}$ mice developed a bleeding diathesis despite the thrombocytosis. This defect was associated with an impaired ability of $Jak2^{Plt-/-}$ platelets to form thrombi under flow and spread onto type 1 collagen. $Jak2^{Plt-/-}$ platelets displayed decreased responses to the collagen receptor GPVI-specific agonist, collagen-related peptide (CRP), including spreading onto fibrinogen, α-granule secretion, integrin αIIbβ3 activation, aggregation, and protein tyrosine phosphorylation. $Jak2^{Plt-/-}$ platelets also displayed mildly attenuated responses to the CLEC-2 agonist rhodocytin. Taken together, the data illustrate a role for the tyrosine kinase JAK2 in platelet immunoreceptor tyrosine-based activation motif (ITAM)/hemITAM signaling that is required for successful in vivo hemostasis.

Materials and methods

Mice

$Jak2^{fl/fl}$ ($Jak2^{Plt+/+}$) mice kindly provided by Kay-Uwe Wagner (Wayne State University) were bred with *Pf4-Cre* mice to generate $Jak2^{fl/fl}$ *Pf4-Cre* ($Jak2^{Plt-/-}$) mice lacking JAK2 in platelets and MKs.[18–21] Mice were treated according to the National Institutes of Health and Medical College of Wisconsin Institutional Animal Care and Use Committee guidelines (Animal Use Application 5600).

Complete blood counts

Mouse blood was collected from the retroorbital plexus and diluted in Cellpack (Sysmex) supplemented with EDTA and PGE_1.[17] Complete blood counts were determined with a Sysmex XT-2000i automatic hematology analyzer, including the immature platelet fraction, which was measured by fluorescent flow cytometry, with proprietary platelet-specific oxazine dyes.

Blood smears

Blood smears were performed with Wright-Giemsa stain. Anticoagulated whole blood was thinly smeared across a glass slide and fixed for 3 minutes in methanol, stained for 1 minute with Wright-Giemsa stain, and washed for 5 minutes in phosphate-buffered saline. Imaging was performed on a Nikon Eclipse E600 microscope equipped with a SPOT insight firewire color mosaic camera (SPOT imaging solutions) and Plan Apo 40×/0.75 objective, with SPOT imaging v5.1.3 software.

Immunohistochemistry

For immunofluorescence microscopy, femurs were stained for GPIbα and laminin and imaged on a Nikon Eclipse Ti2-E platform equipped with a DS-Qi2 camera and Plan Apo 10×/0.45 (NIS-Elements AR 5.02.00 software). Data were image processed with Imaris (Bitplane) and Matlab (MathWorks) software. Additional information is available in the supplemental Methods.

Tail-bleeding time

Bleeding time was determined by snipping 2 mm of distal mouse tail and immediately immersing the tail in 37°C isotonic saline.[22] A complete cessation of bleeding was defined as the bleeding time.

Ferric chloride–induced thrombus formation

Mice were anesthetized and the carotid artery was exposed.[23] A microvascular flow probe (0.5 mm) attached to a transit time perivascular flowmeter (Transonic TS420; AD Instruments) was positioned on the carotid artery to monitor blood flow. Vascular injury was induced by applying a filter paper saturated with 10% ferric chloride ($FeCl_3$) to the top of the vessel for 3 minutes. Blood flow was recorded from immediately after removal of the filter paper until 3 minutes after complete occlusion or a maximal time point of 30 minutes. The time to first occlusion was defined by blood flow of <0.05 mL/min.

Laser-induced thrombus formation

Intravital imaging of the formation of platelet thrombi in mouse cremaster arterioles was performed in the Versiti Blood Research Institute Thrombosis Core Laboratory.[24] Laser intensity and duration were adjusted to produce an injury visible in the brightfield image. Fluorescent images were captured with a high-speed camera (Orca Flash4.0; Hamamatsu). Data were collected for at least 3 minutes after vessel injury. Platelet and fibrin accumulation and/or extravasation confirmed consistent injury. Details are provided in the supplemental Methods.

Ex vivo perfusion assay

Platelet adhesion to immobilized collagen under flow was performed with a microfluidic VenaFlux platform and Vena8Fluor+ biochips (Cellix).[22] An additional description of the procedure is available in the supplemental Methods.

Plasma VWF measurements

Mouse blood was collected by cardiac puncture and anticoagulated in citrate.[25] The plasma Von Willebrand factor (VWF) level was determined by antigen capture enzyme-linked immunosorbent assay

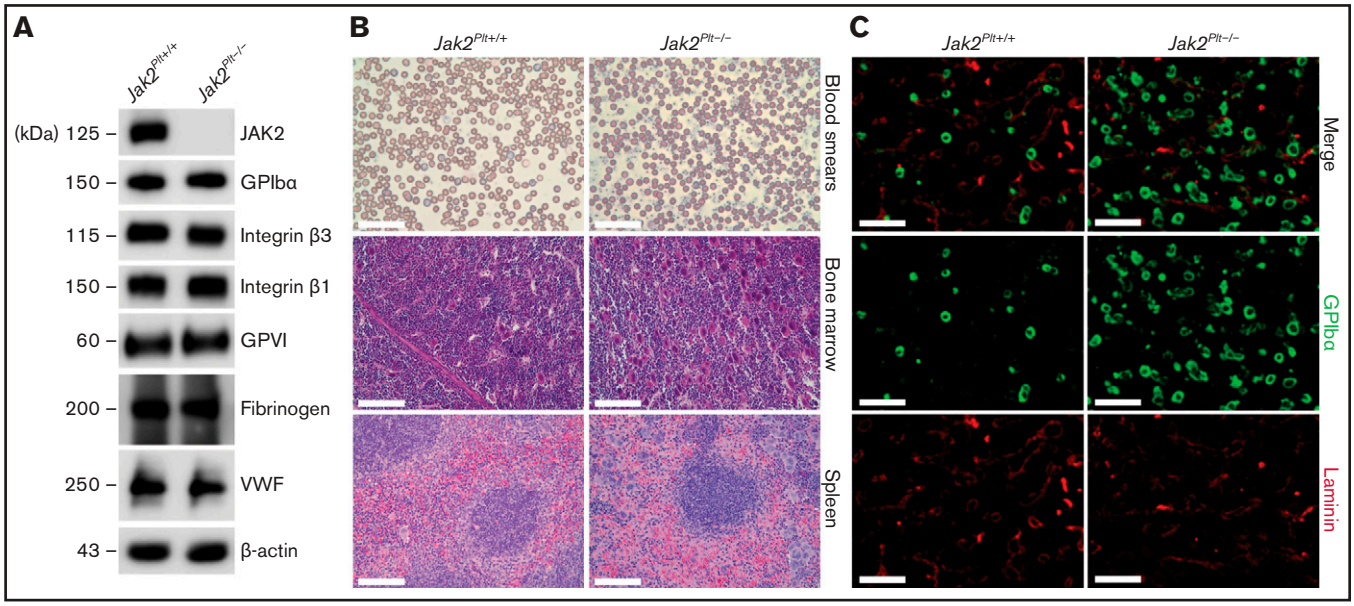

Figure 1. Thrombocytosis and MK hyperplasia in *Jak2*$^{Plt-/-}$ mice. (A) *Jak2*$^{Plt+/+}$ and *Jak2*$^{Plt-/-}$ platelet lysates corresponding to 2 μg of protein were subjected to SDS-PAGE and probed for the proteins indicated, with β-actin as a loading control. Results are representative of 3 independent experiments. (B) Thin blood smears of *Jak2*$^{Plt+/+}$ and *Jak2*$^{Plt-/-}$ mice. Bars represent 40 μm. H&E staining. Bars represent 80 μm. Sections are representative of 3 mice per genotype. (C) Seven-μm-thick femur bone marrow tissue sections from *Jak2*$^{Plt+/+}$ and *Jak2*$^{Plt-/-}$ mice were immunostained for resident MKs and vasculature using anti-GPIbα (488 nm, green) and anti-laminin (568 nm, red) antibodies, respectively, before fluorescent microscopic analysis. Scale bars, 100 μm. Sections shown are representative of 6 mice per genotype.

with monoclonal anti-mouse VWF antibody 344.3 (Versiti) for capture and biotinylated polyclonal anti-VWF (DAKO) for detection. The VWF propeptide (VWFpp) level was determined by antigen capture enzyme-linked immunosorbent assay, with monoclonal anti-VWFpp antibody 349.3 (Versiti) used for capture and biotinylated monoclonal anti-VWFpp antibody 349.2 (Versiti) for detection. A pool of collected C57BL/6J plasma was used as the standard and assigned a value of 1 U/mL.

Platelet preparation

Mouse blood was collected from the retroorbital plexus and anticoagulated in acid citrate dextrose.[22] Platelets were isolated by centrifugation and resuspended at 5×10^8 platelets per milliliter in resuspension buffer (140 mM NaCl, 3 mM KCl, 0.5 mM $MgCl_2$, 5 mM $NaHCO_3$, 10 mM glucose, and 10 mM *N*-2-hydroxyethylpiperazine-*N*′-2-ethanesulfonic acid [pH 7.4]).

Platelet spreading

Samples were imaged on Nikon Structured Illumination Microscopy (N-SIM, NIS-Elements AR v4.40.00 software) and Olympus Confocal FV1000-MPE (FluoView software) platforms under 100× oil objectives. Additional details are available in the supplemental Methods.

Flow cytometry

Platelet surface glycoproteins were investigated by flow cytometry using fluorescently conjugated antibodies: GPIbα, GPIbβ, GPIX, GPV, GPVI (Emfret Analytics), GPIIa, and GPIIIa (BD Biosciences).[26] For VWF binding, washed platelets were incubated in 20% mouse platelet-poor plasma, with or without 4 μg/mL botrocetin (Sigma-Aldrich) for 5 minutes at 37°C and stained with fluorescein isothiocyanate (FITC)-labeled rabbit anti-mouse VWF antibody (Emfret Analytics).[27] For α-granule secretion and αIIbβ3 activation, washed platelets were activated or not with CRP (Versiti Blood Research Institute Protein Chemistry Core Laboratory), rhodocytin (kindly provided by Johannes Eble, University of Münster), human thrombin (Roche), adenosine diphosphate (ADP; Chrono-log), and/or U46619 (Enzo Life Sciences) for 2 minutes at 37°C and stained with FITC-labeled rat anti-mouse P-selectin antibody (BD Biosciences) or Oregon Green 488-labeled fibrinogen (Thermo Fisher Scientific).[22] For αIIbβ3 activation assessment in response to the weak agonists ADP and/or U46619, washed platelets were stimulated for 20 minutes at room temperature in the presence of 1 mM $CaCl_2$ and directly stained with phycoerythrin-labeled anti-active mouse αIIbβ3 antibody JON/A (Emfret Analytics). Fluorescence was quantified with an Accuri C6 flow cytometer (BD Biosciences) and FlowJo software. A total of 20 000 events were analyzed for each sample.

Platelet aggregation

Platelet aggregation was monitored for 5 minutes at 37°C by light transmission under stirring conditions using a Chrono-log Model 490-X aggregometer.

Immunoblot analysis

Platelet proteins were separated by sodium dodecyl sulfate-polyacrylamide gel electrophoresis (SDS-PAGE), transferred onto an Immobilon-P membrane (EMD Millipore), and probed with antibodies directed against the proteins of interest.[22]

Statistical analysis

Results were compared by using the unpaired Student *t* test (mean comparison between 2 groups), 2-way analysis of variance

Table 1. Hematological parameters in *Jak2*$^{Plt-/-}$ mice

Parameter	*Jak2*$^{Plt+/+}$	*Jak2*$^{Plt-/-}$	*P*
Platelets			
Platelets, $10^3/\mu L$	1520 ± 167	7544 ± 1013	<.001
MPV, fL	6.68 ± 0.23	6.73 ± 0.15	.568
IPF, %	4.55 ± 0.66	6.00 ± 1.85	.033
Bone marrow MKs/mm^2	77 ± 18	219 ± 34	<.001
Erythrocytes			
Erythrocytes, $10^3/\mu L$	8500 ± 675	7933 ± 566	.065
MCV, fL	50.58 ± 0.61	51.57 ± 0.88	.011
Reticulocytes, %	2.89 ± 0.63	2.64 ± 0.85	.467
Leukocytes			
Lymphocytes, $10^3/\mu L$	3.78 ± 0.57	5.33 ± 1.99	.050
Granulocytes, $10^3/\mu L$	0.80 ± 0.48	1.27 ± 0.78	.165
Monocytes, $10^3/\mu L$	0.57 ± 0.39	0.87 ± 0.39	.144
Spleen size			
Spleen/body weight, mg/g	2.72 ± 0.53	5.90 ± 1.13	<.001

Results are the means ± SD and are compared by using the unpaired Student *t* test (complete blood count: *Jak2*$^{Plt+/+}$ n = 10 and *Jak2*$^{Plt-/-}$ n = 9; bone marrow MKs: *Jak2*$^{Plt+/+}$ n = 6 and *Jak2*$^{Plt-/-}$ n = 6; spleen size: *Jak2*$^{Plt+/+}$ n = 20 and *Jak2*$^{Plt-/-}$ n = 17). MPV, mean platelet volume; IPF, immature platelet fraction; MKs, megakaryocytes; MCV, mean corpuscular volume.

Table 2. Expression of platelet surface glycoproteins in *Jak2*$^{Plt-/-}$ mice

Glycoprotein	*Jak2*$^{Plt+/+}$	*Jak2*$^{Plt-/-}$	*P*
GPIbα (CD42b)	1 098 ± 448	1 453 ± 323	.091
GPIbβ (CD42c)	3 644 ± 1320	4 650 ± 1486	.174
GPIX (CD42a)	5 835 ± 2341	6 114 ± 876	.757
GPV (CD42d)	1 679 ± 568	1 926 ± 489	.369
GPIIIa (CD61, β3 integrin)	2 257 ± 951	1 971 ± 393	.444
GPIIa (CD29, β1 integrin)	11 051 ± 7521	10 762 ± 5917	.933
GPVI	1 099 ± 240	1 079 ± 203	.861

Glycoprotein surface expression was measured by flow cytometry on freshly isolated *Jak2*$^{Plt+/+}$ and *Jak2*$^{Plt-/-}$ platelets with fluorescence-labeled antibodies. Data are expressed as mean fluorescence intensity. Results represent mean ± SD and are compared by using the unpaired Student *t* test (n = 8 in each group).

(ANOVA; mean comparison between multiple groups), or the log-rank test (survival distribution comparison between 2 groups), with Prism software (GraphPad). Differences were considered statistically significant when $P < .05$.

Results

Thrombocytosis in *Jak2*$^{Plt-/-}$ mice

To investigate the role of JAK2 in platelet hemostatic function, we generated *Jak2*$^{fl/fl}$ *Pf4-Cre* (*Jak2*$^{Plt-/-}$) mice lacking JAK2 in platelets and MKs, as described previously.[17] Loss of JAK2 in *Jak2*$^{Plt-/-}$ platelet lysates was confirmed by immunoblot analysis (Figure 1A). *Jak2*$^{Plt-/-}$ mice developed a severe thrombocytosis with $7544 \times 10^3 \pm 1013 \times 10^3$ platelets per microliter (mean ± standard deviation [SD]; n = 9), compared with $1520 \times 10^3 \pm 167 \times 10^3$ platelets per microliter in *Jak2*$^{Plt+/+}$ littermate controls (n = 10; $P < .001$), a fivefold increase (Table 1). Although the platelets were of normal size, the thrombocytosis was associated with a slight increase in the immature platelet fraction from 4.55% ± 0.66% to 6.00% ± 1.85% ($P = .033$). The erythrocyte count was within normal range, and the leukocyte count, although slightly increased, was not statistically significant. Although they confirmed the thrombocytosis phenotype of the *Jak2*$^{Plt-/-}$ mice, thin blood smears of whole blood did not reveal any notable differences from peripheral blood cell morphology (Figure 1B).

We assessed the surface and total expression of major glycoproteins on *Jak2*$^{Plt-/-}$ platelets by flow cytometry and immunoblot analysis (Figure 1A; Table 2). *Jak2*$^{Plt-/-}$ mice had normal surface expression of all major platelet glycoproteins, and immunoblots of total *Jak2*$^{Plt-/-}$ platelet lysates showed normal fibrinogen and VWF expression, indicative of a normal α-granule cargo.

MK hyperplasia and splenomegaly in *Jak2*$^{Plt-/-}$ mice

Megakaryopoiesis was investigated in *Jak2*$^{Plt-/-}$ and *Jak2*$^{Plt+/+}$ littermate controls by hematoxylin and eosin (H&E) staining and immunofluorescence microscopy. H&E staining revealed an MK expansion in bone marrow sections and throughout the length of the spleen, localized in the peripheral-to-marginal zones of *Jak2*$^{Plt-/-}$ mice (Figure 1B). *Jak2*$^{Plt-/-}$ bone marrow sections had 219 ± 34 MKs per square millimeter (mean ± SD; n = 6), compared with 77 ± 18 MKs per square millimeter in *Jak2*$^{Plt+/+}$ mice (n = 6; $P < .001$), a 2.8-fold increase, as quantified by immunofluorescence microscopy with an antibody directed against MK GPIbα (Figure 1C; Table 1).

Jak2$^{Plt-/-}$ mice displayed severe splenomegaly. At 8 weeks of age, the spleen/body ratio of *Jak2*$^{Plt-/-}$ mice was 5.90 ± 1.13 mg/g (mean ± SD; n = 17), compared with 2.72 ± 0.53 (n = 10; $P < .001$) mg/g in *Jak2*$^{Plt+/+}$ littermate controls, a 2.2-fold increase (Table 1), suggesting extramedullary hematopoiesis.

Bleeding and failure to form stable thrombi in vivo in *Jak2*$^{Plt-/-}$ mice

We evaluated the contribution of platelet JAK2 to hemostasis by using the tail-bleeding–time assay (Figure 2A). Despite the thrombocytosis, *Jak2*$^{Plt-/-}$ mice had a severe bleeding diathesis with a median bleeding time of 8.20 minutes, compared with 2.29 minutes in the *Jak2*$^{Plt+/+}$ littermate controls (n = 10 in each group; log-rank $P = .0108$). In half of the mice, the bleeding continued for 10 minutes, our experimental end point.

To determine whether the prolonged tail bleeding time of *Jak2*$^{Plt-/-}$ mice was related to defective thrombus formation, we next performed a series of in vivo injury models examining thrombosis. We assessed occlusion in *Jak2*$^{Plt-/-}$ mice under high shear flow, by using the $FeCl_3$-induced carotid artery injury model in which the blood flow rate is measured until time to occlusion (Figure 2B-C). In agreement with the observed bleeding diathesis, *Jak2*$^{Plt-/-}$ mice failed to show occlusion up to the experimental end point of 30 minutes, whereas occlusion occurred in *Jak2*$^{Plt+/+}$ littermate controls at a median time of 6.53 minutes (n = 4 in each group; log-rank $P = .0067$; Figure 2B). The pattern of flow during the $FeCl_3$ injury in Figure 2C suggested that the initial formation of thrombi within the artery appeared to dissipate repeatedly, illustrating instability in the developing thrombi, thereby resulting in occlusion failure.

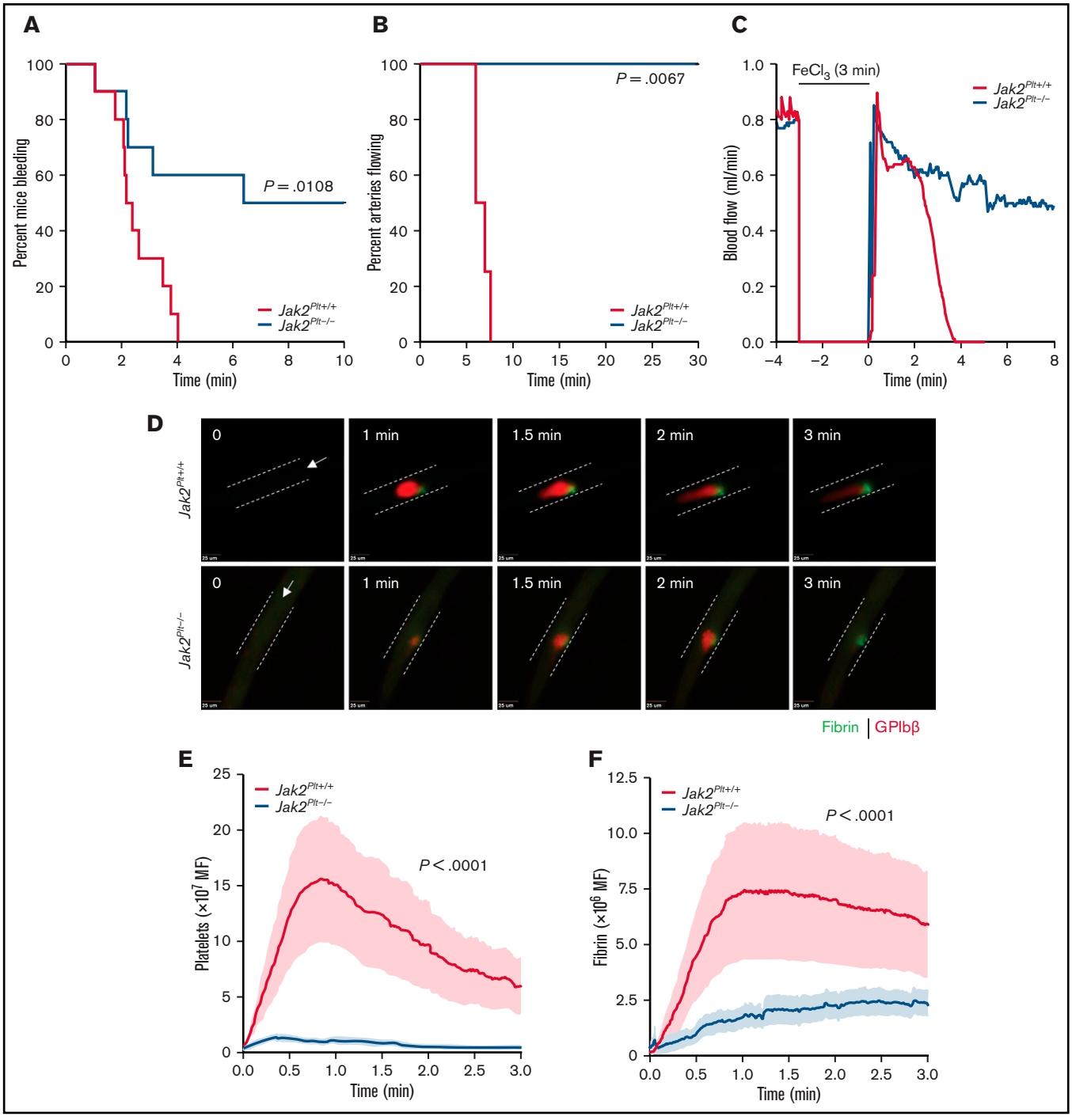

Figure 2. Bleeding and thrombosis defects in *Jak2*$^{Plt-/-}$ mice. (A) Tail-bleeding time of *Jak2*$^{Plt+/+}$ and *Jak2*$^{Plt-/-}$ mice. Results were estimated by the Kaplan-Meier method and were compared by using the log-rank test (n = 10 in each group; log-rank $P = .0108$). (B-C) *Jak2*$^{Plt+/+}$ and *Jak2*$^{Plt-/-}$ mice were exposed to 10% $FeCl_3$ for 3 minutes, and arterial flow rates of the carotid artery were measured with a flow probe up to a maximum of 30 minutes to occlusion. (B) Time to occlusion after $FeCl_3$-induced injury. Results were estimated by the Kaplan-Meier method and were compared by using the log-rank test (n = 4 in each group; log-rank $P = .0067$). (C) Representative blood flow rate graphs. (D-F) Laser-induced injury of the cremaster muscle. *Jak2*$^{Plt+/+}$ and *Jak2*$^{Plt-/-}$ mice were injected with anti-GPIbβ (red) and anti-fibrin (green) antibodies, and the cremaster arteries were interrogated with a 3i Ablate! laser during fluorescence, real-time, intravital video microscopy. (D) Representative still images at 0 to 3 minutes. Arrows represent blood flow direction. Bars represent 25 μm. Platelet (E) and fibrin (F) accumulation at the site of injury was measured by fluorescence intensity. Data are the mean ± standard error of the mean at each time point, compared by using the unpaired Student *t* test (n = 20 vessels in 4 *Jak2*$^{Plt+/+}$ mice and 28 vessels in 5 *Jak2*$^{Plt-/-}$ mice; platelet and fibrin; $P < .0001$).

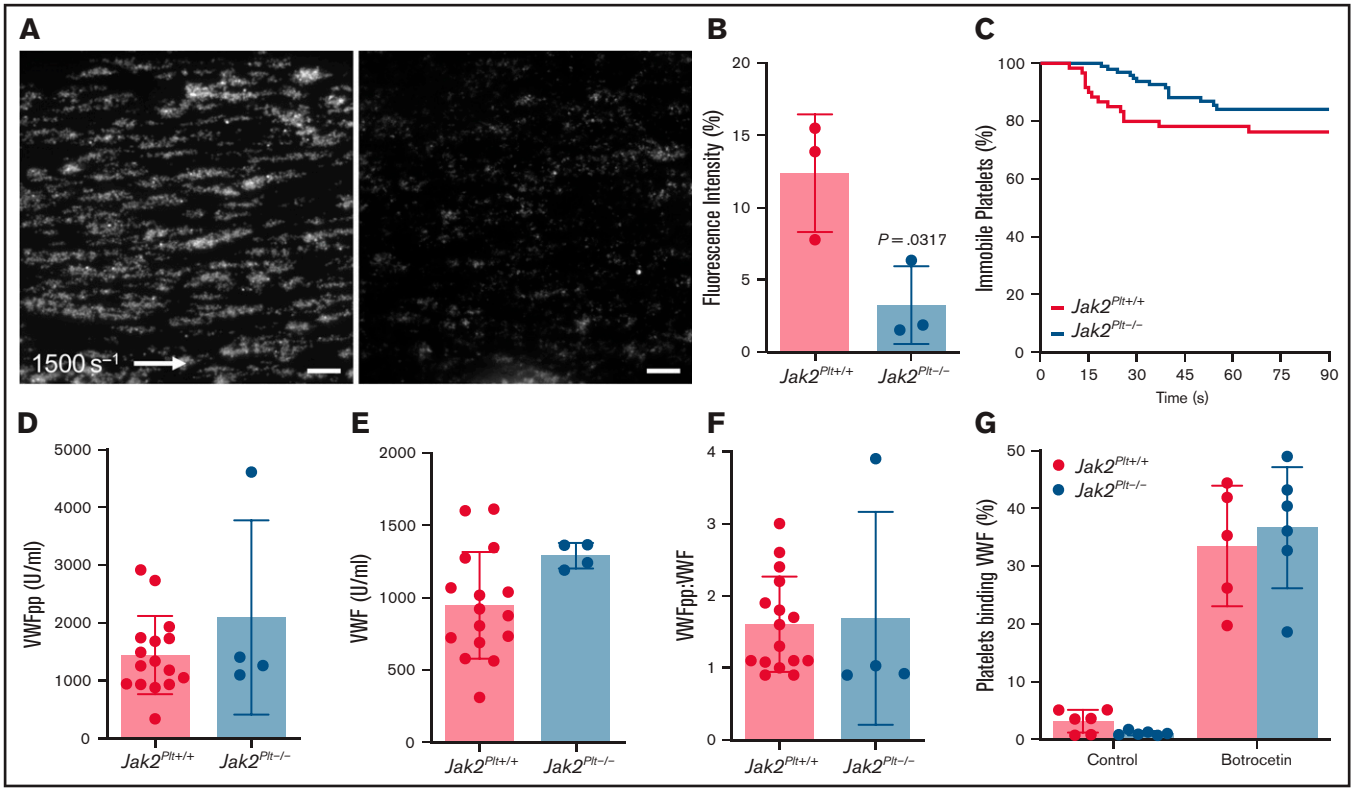

Figure 3. Reduced thrombus formation of *Jak2*$^{Plt-/-}$ platelets at arterial shear rates. PPACK-anticoagulated whole blood from *Jak2*$^{Plt+/+}$ and *Jak2*$^{Plt-/-}$ mice was labeled and perfused on a type 1 collagen–immobilized surface at an arterial shear rate of 1500 s^{-1}. (A) Representative still images at 3 minutes. Bars represent 100 μm. (B) Fluorescence intensity at 3 minutes. Results represent mean ± SD and were compared by using the unpaired Student *t* test (n = 3 in each group; **P* = .0317). (C) Dwell time of individual *Jak2*$^{Plt+/+}$ and *Jak2*$^{Plt-/-}$ platelets. Results were estimated by the Kaplan-Meier method and were compared by using the log-rank test (n = 60 *Jak2*$^{Plt+/+}$ and 97 *Jak2*$^{Plt-/-}$ platelets; log-rank *P* = .141). Plasma VWFpp (D) and VWF (E) levels and VWFpp/VWF ratio (F) in *Jak2*$^{Plt+/+}$ and *Jak2*$^{Plt-/-}$ mice. Results are the mean ± SD and were compared by using the unpaired Student *t* test (n = 16 *Jak2*$^{Plt+/+}$ and 4 *Jak2*$^{Plt-/-}$ mice; VWFpp, *P* = .223; VWF, *P* = .0868; VWFpp/VWF, *P* = .865). (G) *Jak2*$^{Plt+/+}$ and *Jak2*$^{Plt-/-}$ platelets were activated for 5 minutes at 37°C with 4 μg/mL botrocetin, incubated with FITC-labeled anti-mouse VWF antibody, and analyzed by flow cytometry. Results are the mean ± SD and are compared by 2-way ANOVA (n = 6 in each group; control, *P* = .96; botrocetin, *P* = .89).

To investigate the bleeding phenotype in closer detail, we performed a cremaster vessel laser-induced injury model and documented acute thrombus development over 3 minutes (Figure 2D-F; supplemental Videos 1 and 2). The laser-induced injury model enabled us to follow the simultaneous evaluation of platelet accumulation and fibrin deposition in real time. Similar to the $FeCl_3$-induced arterial thrombosis model, platelet accumulation and fibrin deposition were severely decreased at the site of injury in *Jak2*$^{Plt-/-}$ mice, compared with *Jak2*$^{Plt+/+}$ littermate controls (n = 20 vessels in 4 *Jak2*$^{Plt+/+}$ mice and 28 vessels in 5 *Jak2*$^{Plt-/-}$ mice; $P < .0001$ each; Figure 2E-F). Furthermore, *Jak2*$^{Plt-/-}$ mice showed repeated loss of clot aggregation compared with *Jak2*$^{Plt+/+}$ mice (supplemental Videos 1 and 2). Our data demonstrated that JAK2 expression in platelets plays an essential role in platelet thrombus formation in vivo.

Reduced thrombus formation of *Jak2*$^{Plt-/-}$ platelets at arterial shear rates

After blood vessel injury and disruption of the vascular endothelium, platelet exposure to basement membrane proteins and soluble agonists initiates platelet adhesion and activation, leading to formation of thrombi. At arterial shear rates, initial platelet adhesion and subsequent stable activation are mediated by collagen-bound VWF binding to the platelet GPIb-IX complex, followed by platelet activation via the collagen receptor GPVI.[28,29] Using a VenaFlux microfluidics platform,[22] we examined the functionality of fluorescence-labeled *Jak2*$^{Plt-/-}$ platelets in whole blood in adhering to type 1 collagen and forming thrombi under arterial shear rates (1500 s^{-1}; Figure 3A-B). After 3 minutes, the mean fluorescence intensity measured for *Jak2*$^{Plt-/-}$ platelets was 3.25% ± 2.69% (mean ± SD; n = 3), compared with 12.38 ± 4.07% in *Jak2*$^{Plt+/+}$ controls (n = 3; *P* = .0317). We analyzed the dwell time of individual platelets under the same experimental conditions (Figure 3C). *Jak2*$^{Plt+/+}$ (n = 60) and *Jak2*$^{Plt-/-}$ (n = 97) platelets dwelled for similar times (log-rank *P* = .141), suggesting that thrombus formation, rather than initial platelet adhesion, was defective in *Jak2*$^{Plt-/-}$ mice.

Normal VWF levels in *Jak2*$^{Plt-/-}$ plasma

Platelet adhesion at arterial shear rates is dependent on GPIbα-VWF interaction, and hemorrhage in patients with MPN-related thrombocytosis has been associated with increased interaction between platelets and circulating and hemostatically active .VWF.[8,30] Therefore, plasma VWF levels and GPIbα-VWF interactions were assessed to determine their role in the in vivo and in vitro defects in thrombus formation of *Jak2*$^{Plt-/-}$ mice. Compared with *Jak2*$^{Plt+/+}$ controls, *Jak2*$^{Plt-/-}$ mice had normal levels of

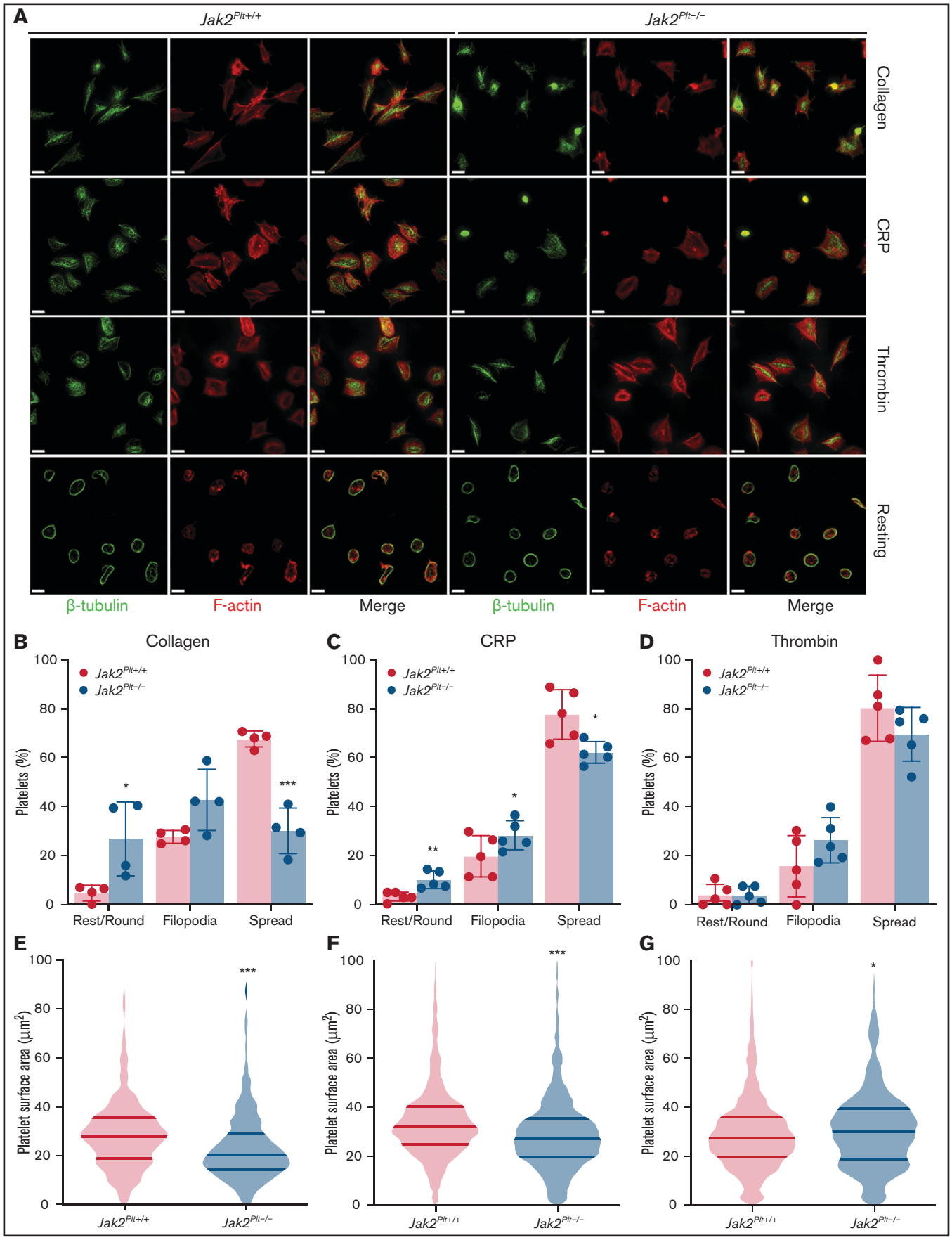

Figure 4.

synthesized VWF propeptide (VWFpp), circulating plasma VWF, and VWF turnover rate (VWFpp/VWF; Figure 3D-F).

To measure platelet GPIbα-VWF interactions, we further performed a flow cytometry–based VWF binding assay after treatment with botrocetin (Figure 3G). The data did not reveal any difference in VWF binding between *Jak2*$^{Plt-/-}$ and *Jak2*$^{Plt+/+}$ control platelets. Together, the data indicate that the bleeding diathesis of *Jak2*$^{Plt-/-}$ mice and failure to form occlusive arterial thrombi was not related to decreased plasma VWF levels or to altered VWF binding to the platelet GPIb-IX complex.

Decreased spreading of *Jak2*$^{Plt-/-}$ platelets

After activation, platelets rapidly change shape from disc-like entities to morphologically distinct forms by rounding, then extending finger-like filopodia and spreading thin sheetlike lamellipodia.[31] To identify whether the reduced thrombus formation of *Jak2*$^{Plt-/-}$ mice was due to defects in platelet shape change, washed platelets were seeded onto glass coverslips coated with 50 μg/mL immobilized type 1 collagen, or were activated with 1 μg/mL of the GPVI agonist CRP or 0.01 U/mL of thrombin and seeded onto 100 μg/mL immobilized fibrinogen (Figure 4A). Unstimulated *Jak2*$^{Plt-/-}$ platelets maintained a normal discoid shape on fibrinogen, as indicated by the presence of their microtubule coil (Figure 4A). We quantified platelet morphology by immunofluorescence staining and superresolution microscopy analysis. On collagen, *Jak2*$^{Plt-/-}$ platelets spread fewer lamellipodia compared with the controls (n = 4 in each group; $P = .0005$), whereas filopodia formation was maintained (Figure 4B). Their surface area moderately decreased to 23.38 ± 14.66 μm^2 (mean ± SD; n = 374), compared with 28.75 ± 15.12 μm^2 in *Jak2*$^{Plt+/+}$ platelets (n = 684; $P < .001$; Figure 4E). *Jak2*$^{Plt-/-}$ platelets activated with CRP on fibrinogen also spread less (n = 5 in each group; $P = .0464$; Figure 4C). Their surface area decreased to 29.68 ± 17.31 μm^2 (mean ± SD; n = 1174), compared with 34.62 ± 17.13 μm^2 in *Jak2*$^{Plt+/+}$ platelets (n = 918; $P < .001$; Figure 4F). By contrast, *Jak2*$^{Plt-/-}$ platelets stimulated with thrombin spread normally on fibrinogen (Figure 4D). Their surface area increased slightly to 31.11 ± 17.29 μm^2 (mean ± SD; n = 842), compared with 29.34 ± 16.15 μm^2 in *Jak2*$^{Plt+/+}$ platelets (n = 958; $P = .03$; Figure 4G). Together, the data suggested a defect downstream of the collagen receptor GPVI.

GPVI-specific functional defects in *Jak2*$^{Plt-/-}$ platelets

We evaluated the function of *Jak2*$^{Plt-/-}$ platelets in response to soluble agonists (Figure 5). We determined P-selectin (CD62P) expression, a marker of α-granule secretion, and fibrinogen binding, a marker of integrin αIIbβ3 activation, after platelet stimulation with CRP (Figure 5A,E), the CLEC-2 agonist rhodocytin (Figure 5B,F) or thrombin (Figure 5C,G) in a dose-dependent manner. As expected, >90% of control platelets expressed P-selectin (Figure 5A-C), and >75% bound fibrinogen (Figure 5E-G) after stimulation at the highest doses of CRP (25 μg/mL), rhodocytin (5 μg/mL), or thrombin (0.5 U/mL). P-selectin exposure and fibrinogen binding were delayed in *Jak2*$^{Plt-/-}$ platelets stimulated with CRP or rhodocytin. Although *Jak2*$^{Plt-/-}$ platelets reached normal P-selectin levels, there was a decrease in fibrinogen binding at maximum CRP concentrations. By contrast, we did not measure differences in tempo and maximum P-selectin expression and fibrinogen binding after thrombin stimulation (Figure 5C,G).

Jak2$^{Plt+/+}$ and *Jak2*$^{Plt-/-}$ platelets were also treated with the G-protein–coupled receptor (GPCR) agonists (ie, ADP and U46619, a thromboxane A2 analogue), and analyzed by flow cytometry for P-selectin expression (Figure 5D) and JON/A binding (Figure 5H), a marker of integrin αIIbβ3 activation. ADP (10 μM) and U46619 (10 μM) induced comparable α-granule secretion and integrin αIIbβ3 activation in *Jak2*$^{Plt+/+}$ and *Jak2*$^{Plt-/-}$ platelets, alone or combined.

Next, we assessed platelet aggregation by light transmission under stirring conditions. *Jak2*$^{Plt-/-}$ platelets aggregated poorly in response to collagen (Figure 5I-K) or a low dose (1 μg/mL) of CRP (Figure 5L) but responded normally to higher doses of CRP (Figure 5M-N) or intermediate doses of thrombin (Figure 5O-P). Together, the data indicate that *Jak2*$^{Plt-/-}$ platelets have impaired α-granule secretion, integrin αIIbβ3 activation, and aggregation when stimulated via the ITAM/hemITAM-containing receptors GPVI and CLEC-2, but not when activated with the GPCR agonists thrombin, ADP, and U46619.

Impaired GPVI signaling in *Jak2*$^{Plt-/-}$ platelets

Collagen binding to platelet GPVI initiates an ITAM signaling cascade that involves the stepwise activation and phosphorylation of several of the signaling intermediates, beginning with the proximal Src family tyrosine kinases (SFKs) Fyn and Lyn.[32] Activation of SFKs subsequently induces phosphorylation of other signaling intermediates, including the GPVI-associated FcRγ-chain, the tyrosine kinase Syk, and phospholipase C-γ2 (PLC-γ2). We wanted to determine whether the collagen- and CRP-related defects of *Jak2*$^{Plt-/-}$ platelets were due to impaired ITAM signaling downstream of GPVI. We activated platelets with increasing CRP concentrations and lysed and probed against phosphotyrosine (pTyr; Figure 6A). In control *Jak2*$^{Plt+/+}$ platelets, CRP stimulation induced the tyrosine phosphorylation of several proteins, whereas *Jak2*$^{Plt-/-}$ platelets showed an attenuated response in protein tyrosine phosphorylation.

To further refine the signaling impairment, we probed CRP-stimulated platelet lysates for activating phosphorylated tyrosine residues on Lyn (Tyr396), Syk (Tyr525/526), and PLC-γ2 (Tyr1217) using phospho-specific antibodies (Figure 6A). *Jak2*$^{Plt-/-}$ platelets

Figure 4. Spreading defects in *Jak2*$^{Plt-/-}$ platelets. *Jak2*$^{Plt+/+}$ and *Jak2*$^{Plt-/-}$ platelets were left to adhere to 50 μg/mL type 1 collagen or to 100 μg/mL fibrinogen and activated with 1 μg/mL CRP or 0.01 U/mL thrombin glass coverslips for 30 minutes at 37°C as indicated. Fixed platelets were stained for β-tubulin and F-actin (phalloidin) and analyzed by structured illumination microscopy. (A) Representative immunofluorescent micrographs of fixed platelets. Bars represent 3 μm (activated) and 7 μm (resting). (B-D) Morphologic quantification of platelet spreading as determined by resting, extension of defined filopodia, or full spreading in response to collagen (total platelets scored, 549 *Jak2*$^{Plt+/+}$ and 311 *Jak2*$^{Plt-/-}$ in 4 independent experiments) (B); CRP (total platelets scored, 888 *Jak2*$^{Plt+/+}$ and 1017 *Jak2*$^{Plt-/-}$ in 5 independent experiments) (C); or thrombin (total platelets scored, 932 *Jak2*$^{Plt+/+}$ and 796 *Jak2*$^{Plt-/-}$ in 5 independent experiments) (D). Results represent the mean ± SD and were compared by 2-way ANOVA. *$P < .05$; **$P < .01$; ***$P < .001$. (E-G) Violin plots of platelet surface area in response to collagen (total platelets scored, 684 *Jak2*$^{Plt+/+}$ and 374 *Jak2*$^{Plt-/-}$ in 4 independent experiments) (E); CRP (total platelets scored, 918 *Jak2*$^{Plt+/+}$ and 1174 *Jak2*$^{Plt-/-}$ in 5 independent experiments) (F); or thrombin (total platelets scored, 958 *Jak2*$^{Plt+/+}$ and 842 *Jak2*$^{Plt-/-}$ in 5 independent experiments) (G). Results were compared by 2-way ANOVA. *$P < .05$; ***$P < .001$.

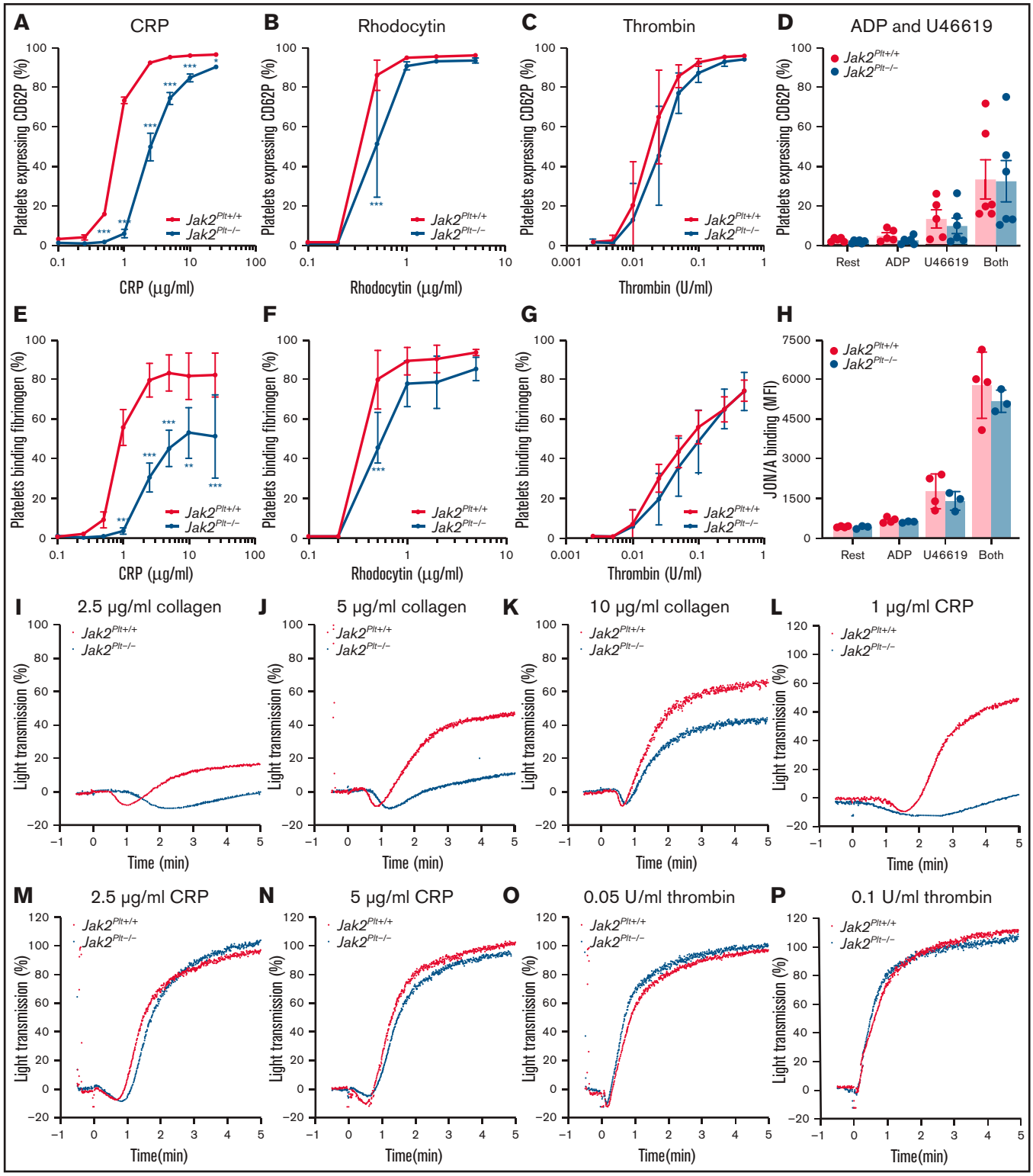

Figure 5. Functional defects of *Jak2*$^{Plt-/-}$ platelets downstream of GPVI and CLEC-2. *Jak2*$^{Plt+/+}$ and *Jak2*$^{Plt-/-}$ platelets were activated for 2 minutes at 37°C with CRP (A,E), rhodocytin (B,F), thrombin (C,G), or ADP and U46619 (D,H); incubated with FITC-labeled anti-mouse CD62P antibody (A-D), Oregon Green 488-labeled fibrinogen (E-G), or anti-active αIIbβ3 antibody JON/A (H); and analyzed by flow cytometry. Results are expressed as a percentage of positive platelets (A-G) or mean fluorescence intensity (MFI) (H). Results represent mean ± SD of 5 (CRP), 4 (rhodocytin), 6 (thrombin), and 4 (ADP and U46619) independent experiments and were compared by 2-way ANOVA. $^{*}P < .05$; $^{**}P < .01$; $^{***}P < .001$. Aggregation of *Jak2*$^{Plt+/+}$ and *Jak2*$^{Plt-/-}$ platelets was determined by light transmission under stirring conditions at 37°C in response to 2.5 (I), 5 (J), or 10 (K) μg/mL collagen; 1 (L), 2.5 (M), or 5 (N) μg/mL CRP; or 0.05 (O) or 0.1 (P) U/mL thrombin. Graphs are representative of 4 independent experiments.

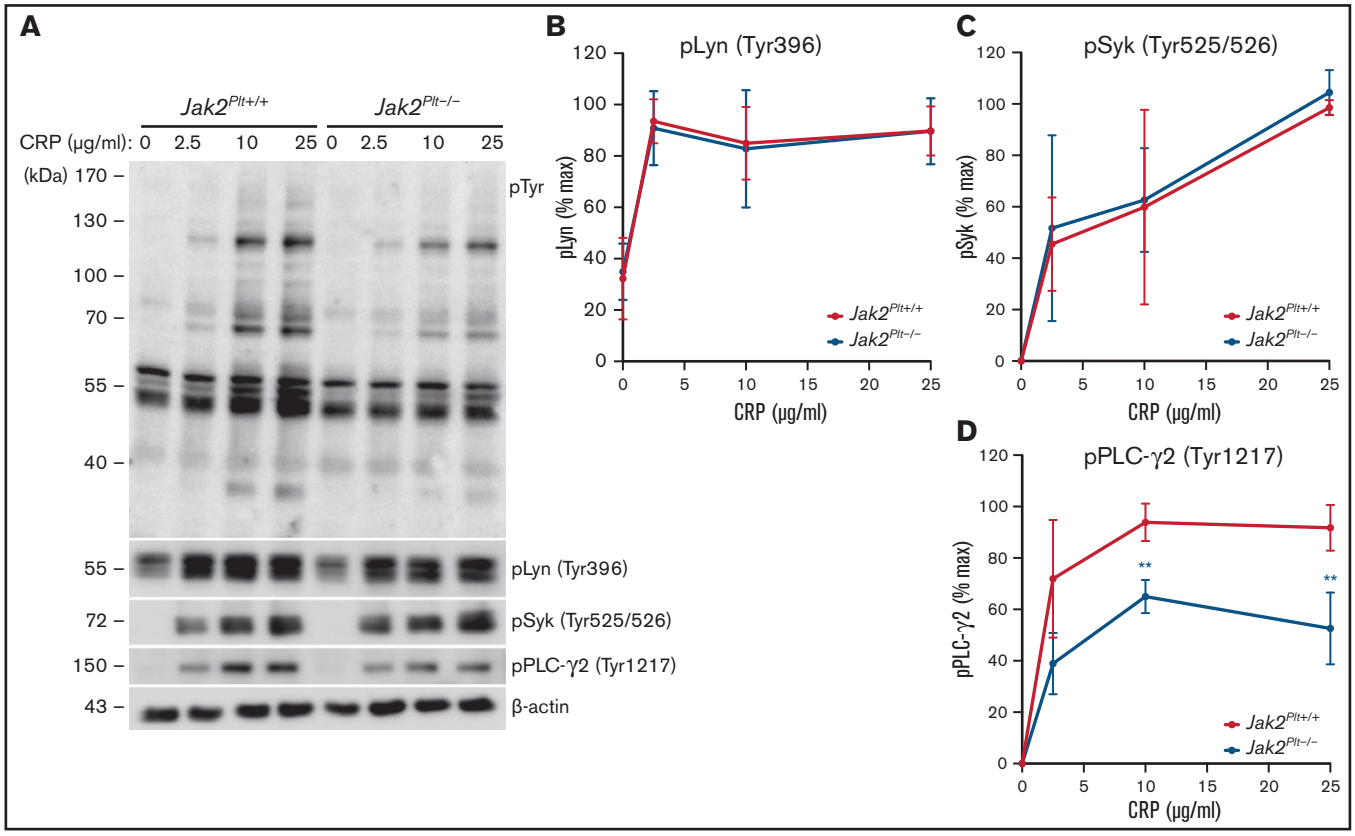

Figure 6. GPVI signaling defects in *Jak2*$^{Plt-/-}$ platelets. (A) *Jak2*$^{Plt+/+}$ and *Jak2*$^{Plt-/-}$ platelets were activated or not with CRP for 2 minutes at 37°C, as indicated. Platelet lysates corresponding to 2 μg protein were subjected to SDS-PAGE and probed for phosphotyrosine (pTyr), phosphorylated Lyn Tyr 396 (pLyn Tyr396), phosphorylated Syk Tyr525/526 (pSyk Tyr525/526), phosphorylated PLC-γ2 Tyr1217 (pPLC-γ2 Tyr1217), and β-actin as a loading control. Quantification of pLyn Tyr396 (B), pSyk Tyr525/526 (C), and pPLCγ2 Tyr1217 (D) in CRP-stimulated *Jak2*$^{Plt+/+}$ and *Jak2*$^{Plt-/-}$ platelets. Results are the mean ± SD of 4 independent experiments and were compared with the control by 2-way ANOVA. $^{**}P < .01$.

showed comparable phosphorylation of Lyn (Tyr396) (Figure 6B) and Syk (Tyr525/526) (Figure 6C) to control *Jak2*$^{Plt+/+}$ platelets. Notably, levels of phosphorylated PLC-γ2 at its activating residue Tyr1217 were reduced by 30% at 10 μg/mL and by 40% at 25 μg/mL of CRP (Figure 6D). The data show that the absence of JAK2-mediated signals did not affect the early signaling intermediates Lyn and Syk downstream of GPVI, but affected other downstream signaling intermediates, leading to impaired PLC-γ2 phosphorylation and activation.

Discussion

The cellular mechanisms by which somatic mutations in the tyrosine kinase JAK2 increase the risk of developing arterial and venous thrombosis in patients with MPNs remain unclear. In this study, we examined the role of platelet JAK2 in primary hemostasis using *Jak2*$^{Plt-/-}$ mice lacking JAK2 in platelets and MKs and described a novel mechanism by which platelet JAK2 contributes to thrombosis in mice.

Jak2$^{Plt-/-}$ mice had severe MK hyperplasia and thrombocytosis.[17] Previous studies have linked the endocytosis of the TPO receptor Mpl and regulation of plasma TPO by platelets to JAK2 expression and activity and Mpl and JAK2 protein levels to MK proliferation.[33-35] *Jak2*$^{Plt-/-}$ mice have elevated plasma TPO levels caused by defective endocytosis of the cytokine by platelets and MKs.[17] Mouse models lacking Mpl, the endocytic GTPase dynamin 2, or the ubiquitin ligase Cbl in platelets and MKs, where blunted TPO endocytosis results in hemapoietic stem and progenitor cell and MK hyperplasia related to increased TPO stimulation, support the role of Mpl-mediated endocytosis regulating TPO plasma levels.[26,36,37]

Thrombocytosis is typically associated with thrombosis and thrombocytopenia with bleeding. Thus, the most confounding observation was the severe tail-bleeding diathesis and hemostatic defects of *Jak2*$^{Plt-/-}$ mice. By 2 independent in vivo mouse models of thrombosis, we demonstrated that JAK2 expression in platelets contributes to primary hemostasis. Occlusion failed in *Jak2*$^{Plt-/-}$ mice in a $FeCl_3$-induced arterial injury model, which was associated with development of unstable thrombus, and no stable thrombi were created in a cremaster laser–induced injury system, in which *Jak2*$^{Plt-/-}$ platelets did not successfully stabilize at the site of vascular injury. The genetic approach of deleting JAK2 in platelets is consistent with earlier reports of a pharmacological approach, where treatment with the specific JAK2 inhibitor AG490 also led to prolonged microvessel occlusion time in mice.[38] Hemostatic defects have been observed in knockin mouse models expressing the hyperactive

JAK2 V617F in platelets.[15,16] Why loss of JAK2 function, related to genetic deletion or pharmacological inhibition, and expression of hyperactive *JAK2* V617F in platelets may lead to similar in vivo and in vitro hemostatic defects remains unexplained.

Under arterial shear rates, the initial platelet adhesion to subendothelial collagen is mediated by collagen-induced VWF binding to the platelet GPIb-IX complex, and subsequent activation of platelet collagen receptor GPVI.[28,29] *Jak2*$^{Plt-/-}$ platelets had thrombus formation defects after normal adhesion to immobilized type 1 collagen under arterial shear rates. *Jak2*$^{Plt-/-}$ mice had normal plasma ppVWF and VWF plasma levels, and *Jak2*$^{Plt-/-}$ platelets expressed the GPIb-IX complex and the collagen receptor GPVI normally. Furthermore, plasma VWF binding to *Jak2*$^{Plt-/-}$ platelets in response to botrocetin was indistinguishable from controls. The data show that the interaction between plasma VWF and the platelet GPIb-IX complex was not disrupted by JAK2 deletion in platelets. By contrast, *Jak2*$^{Plt-/-}$ platelet spreading was impaired on immobilized collagen or fibrinogen after the addition of low doses of the collagen receptor GPVI agonist CRP, but not thrombin. Together, our data suggest that in vivo hemostatic defects and consequent bleeding of *Jak2*$^{Plt-/-}$ mice is not caused by defective VWF and GPIbα-VWF interactions, but is the result of defective platelet activation in response to collagen exposure, a critical initial step in thrombus development.

Supporting a role for JAK2 in intrinsic platelet GPVI signaling and function, we identified defects in the ability of *Jak2*$^{Plt-/-}$ platelets to secrete α-granule, activate integrin αIIbβ3, and aggregate in response to exposure collagen and CRP, but not in response to the GPCR agonists, thrombin, ADP, and the thromboxane A2 analogue U46619. The GPVI-specific impairments of *Jak2*$^{Plt-/-}$ platelets observed are consistent with previous observations showing that pharmacological JAK2 inhibition results in impaired platelet aggregation after stimulation by collagen, but not by thrombin.[38] The contribution of ADP release from dense granules and thromboxane A2 formation in the responses of *Jak2*$^{Plt-/-}$ platelets to GPVI agonists was not evaluated in our study and cannot be ruled out, as ADP scavengers and aspirin affect, to various degrees, platelet responses to collagen, CRP, and convulxin.[39-41] Elegant studies using an in vivo platelet depletion model have shown that newly formed young platelets display GPVI signaling defects.[42] Although a minimal increase in immature platelet fraction was observed in *Jak2*$^{Plt-/-}$ mice, impaired GPVI signaling in this fraction alone is unlikely to be responsible for the hemostatic defects, as most *Jak2*$^{Plt-/-}$ platelets are mature and circulate normally.[17]

Additional support for the role of GPVI in the hemostatic defect of in *Jak2*$^{Plt-/-}$ platelets came from the reduced intracellular protein tyrosine phosphorylation in response to CRP. The absence of JAK2-mediated signals did not affect the early downstream GPVI signaling kinases Lyn and Syk but showed impaired phosphorylation of PLC-γ2. Thus, our data posit a role for JAK2 on unidentified signaling intermediates downstream of Syk and upstream of PLC-γ2. The phenotype of *Jak2*$^{Plt-/-}$ mice resembles that of mice lacking PLC-γ2,[43] which is activated downstream of both GPVI and the hemITAM receptor CLEC-2. Because GPVI and the CLEC-2 share many signaling molecules, it is likely that JAK2 also affects CLEC-2 signaling. Consistent with the hypothesis, α-granule secretion, and integrin αIIbβ3 activation were mildly attenuated in *Jak2*$^{Plt-/-}$ platelets stimulated with the CLEC-2 agonist rhodocytin. Phosphoproteomics-based studies have identified JAK2 tyrosine phosphorylation downstream of both GPVI and CLEC-2.[44,45] In addition, Mpl/JAK2 signaling may also contribute to the regulation of platelet hemostatic function in vivo, as TPO potentiates GPVI signaling through a phosphatidylinositol 3-kinase–dependent pathway in human platelets.[46,47] Potentiation of platelet GPVI signaling by TPO is lost in platelets of *JAK2* V617F patients.[48] Mice expressing the activating *JAK2* V617F mutation also develop platelet hemostatic defects, further supporting this notion.[15,16] Thus, combined GPVI, CLEC-2, and Mpl signaling defects likely explain the bleeding diathesis of *Jak2*$^{Plt-/-}$ mice.

In conclusion, although our study identified a role for the tyrosine kinase JAK2 in platelet GPVI and CLEC-2 signaling that is necessary for successful in vivo hemostasis in mice, the contribution of other JAK2 signaling-dependent receptors should be investigated further.

Acknowledgments

The authors thank Kay-Uwe Wagner for providing the *Jak2*$^{fl/fl}$ mice, Johannes Eble for providing the rhodocytin, François Maignen for statistical expertise, and Karin Hoffmeister for helpful discussions.

This work was supported by National Institutes of Health, National Heart, Lung, and Blood Institute R01 grants HL136430 (S.L.H.), HL133348 (H.W.), and HL126743 (H.F.).

Authorship

Contribution: N.E. designed and performed experiments, collected, analyzed, and interpreted data, and wrote and revised the manuscript; S.S., M.L.S., C.D., and D.J. designed and performed the experiments; collected, analyzed, and interpreted the data; and revised the manuscript; S.L.H. and H.W. analyzed and interpreted data and revised the manuscript; and H.F. conceived and designed the study, designed and performed experiments, collected, analyzed, and interpreted the data and wrote and revised the manuscript.

Conflict-of-interest disclosure: The authors declare no competing financial interests.

The current affiliation for S.S. is Department of Medicine, Boston University School of Medicine, Boston, MA.

ORCID profiles: N.E., 0000-0001-9479-1365; S.S., 0000-0002-0194-5044; S.L.H., 0000-0002-5545-8014; H.W., 0000-0003-4034-4249; H.F., 0000-0003-0788-9204.

Correspondence: Hervé Falet, Versiti Blood Research Institute, 8733 W Watertown Plank Rd, Milwaukee, WI 53226; e-mail: hfalet@versiti.org.

References

1. Vainchenker W, Constantinescu SN. JAK/STAT signaling in hematological malignancies. *Oncogene.* 2013;32(21):2601-2613.
2. Rawlings JS, Rosler KM, Harrison DA. The JAK/STAT signaling pathway. *J Cell Sci.* 2004;117(Pt 8):1281-1283.

3. Tefferi A. Novel mutations and their functional and clinical relevance in myeloproliferative neoplasms: JAK2, MPL, TET2, ASXL1, CBL, IDH and IKZF1. *Leukemia.* 2010;24(6):1128-1138.
4. Tefferi A. Mutational analysis in BCR-ABL-negative classic myeloproliferative neoplasms: impact on prognosis and therapeutic choices. *Leuk Lymphoma.* 2010;51(4):576-582.
5. Wan X, Ma Y, McClendon CL, Huang LJ, Huang N. Ab initio modeling and experimental assessment of Janus Kinase 2 (JAK2) kinase-pseudokinase complex structure. *PLOS Comput Biol.* 2013;9(4):e1003022.
6. Rumi E, Pietra D, Pascutto C, et al; Associazione Italiana per la Ricerca sul Cancro Gruppo Italiano Malattie Mieloproliferative Investigators. Clinical effect of driver mutations of JAK2, CALR, or MPL in primary myelofibrosis. *Blood.* 2014;124(7):1062-1069.
7. Landolfi R, Marchioli R, Kutti J, et al; European collaboration on low-dose aspirin in polycythemia vera investigators. Efficacy and safety of low-dose aspirin in polycythemia vera. *N Engl J Med.* 2004;350(2):114-124.
8. Elliott MA, Tefferi A. Thrombosis and haemorrhage in polycythaemia vera and essential thrombocythaemia. *Br J Haematol.* 2005;128(3):275-290.
9. Tefferi A, Elliott M. Thrombosis in myeloproliferative disorders: prevalence, prognostic factors, and the role of leukocytes and JAK2V617F. *Semin Thromb Hemost.* 2007;33(4):313-320.
10. Finazzi G, Rambaldi A, Guerini V, Carobbo A, Barbui T. Risk of thrombosis in patients with essential thrombocythemia and polycythemia vera according to JAK2 V617F mutation status. *Haematologica.* 2007;92(1):135-136.
11. Lussana F, Caberlon S, Pagani C, Kamphuisen PW, Büller HR, Cattaneo M. Association of V617F Jak2 mutation with the risk of thrombosis among patients with essential thrombocythaemia or idiopathic myelofibrosis: a systematic review. *Thromb Res.* 2009;124(4):409-417.
12. Campbell PJ, Scott LM, Buck G, et al; Australasian Leukaemia and Lymphoma Group. Definition of subtypes of essential thrombocythaemia and relation to polycythaemia vera based on JAK2 V617F mutation status: a prospective study. *Lancet.* 2005;366(9501):1945-1953.
13. Hobbs CM, Manning H, Bennett C, et al. JAK2V617F leads to intrinsic changes in platelet formation and reactivity in a knock-in mouse model of essential thrombocythemia. *Blood.* 2013;122(23):3787-3797.
14. Etheridge SL, Roh ME, Cosgrove ME, et al. JAK2V617F-positive endothelial cells contribute to clotting abnormalities in myeloproliferative neoplasms. *Proc Natl Acad Sci USA.* 2014;111(6):2295-2300.
15. Lamrani L, Lacout C, Ollivier V, et al. Hemostatic disorders in a JAK2V617F-driven mouse model of myeloproliferative neoplasm. *Blood.* 2014;124(7):1136-1145.
16. Matsuura S, Thompson CR, Belghasem ME, et al. Platelet dysfunction and thrombosis in JAK2^{V617F}-mutated primary myelofibrotic mice. *Arterioscler Thromb Vasc Biol.* 2020;40(10):e262-e272.
17. Meyer SC, Keller MD, Woods BA, et al. Genetic studies reveal an unexpected negative regulatory role for Jak2 in thrombopoiesis. *Blood.* 2014;124(14):2280-2284.
18. Krempler A, Qi Y, Triplett AA, Zhu J, Rui H, Wagner KU. Generation of a conditional knockout allele for the Janus kinase 2 (Jak2) gene in mice. *Genesis.* 2004;40(1):52-57.
19. Wagner KU, Krempler A, Triplett AA, et al. Impaired alveologenesis and maintenance of secretory mammary epithelial cells in Jak2 conditional knockout mice. *Mol Cell Biol.* 2004;24(12):5510-5520.
20. Tiedt R, Schomber T, Hao-Shen H, Skoda RC. Pf4-Cre transgenic mice allow the generation of lineage-restricted gene knockouts for studying megakaryocyte and platelet function in vivo. *Blood.* 2007;109(4):1503-1506.
21. Lorenz V, Ramsey H, Liu ZJ, et al. Developmental stage-specific manifestations of absent TPO/c-MPL signalling in newborn mice. *Thromb Haemost.* 2017;117(12):2322-2333.
22. Eaton N, Drew C, Wieser J, Munday AD, Falet H. Dynamin 2 is required for GPVI signaling and platelet hemostatic function in mice. *Haematologica.* 2020;105(5):1414-1423.
23. Subramaniam S, Kanse SM. Ferric chloride-induced arterial thrombosis in mice. *Curr Protoc Mouse Biol.* 2014;4(4):151-164.
24. Gao J, Huang M, Lai J, et al. Kindlin supports platelet integrin αIIbβ3 activation by interacting with paxillin. *J Cell Sci.* 2017;130(21):3764-3775.
25. Jacobi PM, Kanaji S, Jakab D, Gehrand AL, Johnsen JM, Haberichter SL. von Willebrand factor propeptide to antigen ratio identifies platelet activation and reduced von Willebrand factor survival phenotype in mice. *J Thromb Haemost.* 2018;16(3):546-554.
26. Bender M, Giannini S, Grozovsky R, et al. Dynamin 2-dependent endocytosis is required for normal megakaryocyte development in mice. *Blood.* 2015;125(6):1014-1024.
27. Giannini S, Lee-Sundlov MM, Rivadeneyra L, et al. β4GALT1 controls β1 integrin function to govern thrombopoiesis and hematopoietic stem cell homeostasis. *Nat Commun.* 2020;11(1):356.
28. Goto S, Tamura N, Handa S, Arai M, Kodama K, Takayama H. Involvement of glycoprotein VI in platelet thrombus formation on both collagen and von Willebrand factor surfaces under flow conditions. *Circulation.* 2002;106(2):266-272.
29. Nieswandt B, Watson SP. Platelet-collagen interaction: is GPVI the central receptor? *Blood.* 2003;102(2):449-461.
30. Budde U, Scharf RE, Franke P, Hartmann-Budde K, Dent J, Ruggeri ZM. Elevated platelet count as a cause of abnormal von Willebrand factor multimer distribution in plasma. *Blood.* 1993;82(6):1749-1757.
31. Falet H. Anatomy of the Platelet Cytoskeleton. In: Gresele P, Kleiman NS, López JA, Page CP, et al. eds. Platelets in thrombotic and non-thrombotic disorders: pathophysiology, pharmacology and therapeutics: an update. Cham, Switzerland: Springer International Publishing; 2017:139-156.

32. Watson SP, Auger JM, McCarty OJ, Pearce AC. GPVI and integrin alphaIIb β3 signaling in platelets. *J Thromb Haemost.* 2005;3(8):1752-1762.

33. Royer Y, Staerk J, Costuleanu M, Courtoy PJ, Constantinescu SN. Janus kinases affect thrombopoietin receptor cell surface localization and stability. *J Biol Chem.* 2005;280(29):27251-27261.

34. Pecquet C, Diaconu CC, Staerk J, et al. Thrombopoietin receptor down-modulation by JAK2 V617F: restoration of receptor levels by inhibitors of pathologic JAK2 signaling and of proteasomes. *Blood.* 2012;119(20):4625-4635.

35. Besancenot R, Roos-Weil D, Tonetti C, et al. JAK2 and MPL protein levels determine TPO-induced megakaryocyte proliferation vs differentiation. *Blood.* 2014;124(13):2104-2115.

36. Ng AP, Kauppi M, Metcalf D, et al. Mpl expression on megakaryocytes and platelets is dispensable for thrombopoiesis but essential to prevent myeloproliferation. *Proc Natl Acad Sci USA.* 2014;111(16):5884-5889.

37. Märklin M, Tandler C, Kopp HG, et al. C-Cbl regulates c-MPL receptor trafficking and its internalization. *J Cell Mol Med.* 2020;24(21):12491-12503.

38. Lu WJ, Lin KC, Huang SY, et al. Role of a Janus kinase 2-dependent signaling pathway in platelet activation. *Thromb Res.* 2014;133(6):1088-1096.

39. Atkinson BT, Stafford MJ, Pears CJ, Watson SP. Signalling events underlying platelet aggregation induced by the glycoprotein VI agonist convulxin. *Eur J Biochem.* 2001;268(20):5242-5248.

40. Quinton TM, Ozdener F, Dangelmaier C, Daniel JL, Kunapuli SP. Glycoprotein VI-mediated platelet fibrinogen receptor activation occurs through calcium-sensitive and PKC-sensitive pathways without a requirement for secreted ADP. *Blood.* 2002;99(9):3228-3234.

41. Leunissen TC, Wisman PP, van Holten TC, et al. The effect of P2Y12 inhibition on platelet activation assessed with aggregation- and flow cytometry-based assays. *Platelets.* 2017;28(6):567-575.

42. Gupta S, Cherpokova D, Spindler M, Morowski M, Bender M, Nieswandt B. GPVI signaling is compromised in newly formed platelets after acute thrombocytopenia in mice. *Blood.* 2018;131(10):1106-1110.

43. Nonne C, Lenain N, Hechler B, et al. Importance of platelet phospholipase Cgamma2 signaling in arterial thrombosis as a function of lesion severity. *Arterioscler Thromb Vasc Biol.* 2005;25(6):1293-1298.

44. Izquierdo I, Barrachina MN, Hermida-Nogueira L, et al. A comprehensive tyrosine phosphoproteomic analysis reveals novel components of the platelet CLEC-2 signaling cascade. *Thromb Haemost.* 2020;120(2):262-276.

45. Babur Ö, Melrose AR, Cunliffe JM, et al. Phosphoproteomic quantitation and causal analysis reveal pathways in GPVI/ITAM-mediated platelet activation programs. *Blood.* 2020;136(20):2346-2358.

46. Rodríguez-Liñares B, Watson SP. Thrombopoietin potentiates activation of human platelets in association with JAK2 and TYK2 phosphorylation. *Biochem J.* 1996;316(Pt 1):93-98.

47. Pasquet JM, Gross BS, Gratacap MP, et al. Thrombopoietin potentiates collagen receptor signaling in platelets through a phosphatidylinositol 3-kinase-dependent pathway. *Blood.* 2000;95(11):3429-3434.

48. Moore SF, Hunter RW, Harper MT, et al. Dysfunction of the PI3 kinase/Rap1/integrin α(IIb)β(3) pathway underlies ex vivo platelet hypoactivity in essential thrombocythemia. *Blood.* 2013;121(7):1209-1219.